RESEARCH ON THE AIRCRAFT NOSE WHEEL STEERING SYSTEM'S SIMULATION AND FAULT ANALYSIS

Xudong SHI[1*], Xinjie CHANG[1], Xu WANG[2], Fujun YING[1]

In the design of the aircraft system, the verification of the system is the most important step. To meet the airworthiness requirements, it is necessary to verify the performance of the nose wheel steering system during the design verification stage. Because of the design cost and verification efficiency, instead of doing the system level test directly with the hardware setup, it is meaningful to implement certain pre-verification using simulation model in advance. Therefore, the AMESim platform was used to model the entire nose wheel steering system, including the mechanical part and the electrical part. The model can be used to simulate the whole landing gear steering process, then various intermediate parameters can be collected and analyzed for performance verification. In addition, different faults are modeled and injected, then the consequential impact is analyzed by the detailed simulation parameters.

Keywords: Aircraft nose wheel; Steering system; System simulation; Fault analysis

1. Introduction

Verification of the system is one of the most important steps in the design of the aircraft system, which is of great importance to the safe operation of the aircraft. Therefore, not only the verification of the systems related to the aircraft steering system needs to be completed, but also the verification of the inter-system of the steering system. For the verification of inter-system, the establishment of the simulation system is significant to reduce the cost and improve the efficiency of verification. The simulation of aircraft steering system is established, which can be jointly debugged with the simulation of relevant systems under their normal state. When aircraft steering system have failures, joint debugging is necessary for the verification of related systems. Then the failure causes of the steering system are analyzed and the electrical signals trend are simulated. This is of great significance to the verification of the related systems in the future.

At present, many scholars have made relevant researches on modeling and simulation of aircraft nose wheel steering system. Pavan et al. used

[1] College of Electronic Information and Automation, Civil Aviation University of China, Tianjin, China
[2] Aircraft Maintenance and Engineering Corporation, Beijing, China

Matlab/Simulink simulation platform to simulate the aircraft nose wheel steering system [1]. Robert used ADAMS to model the aircraft nose wheel steering system, and injected the fault factors that caused the aircraft steering failure into the model for analysis [2]. For the analysis of the factors affecting the failure of the aircraft nose wheel steering system, many scholars have also made relevant research. Mohsen et al. studied the effect of coulomb friction, a key parameter that causes the occurrence and type of the nose landing gear swing [3]. Infante et al. uses the finite element method to analyze the failure devices of the aircraft nose landing gear in detail [4]. Hu et al. analyzed the cause of failure of oil leakage failure of aircraft nose wheel steering actuator [5].

2. Modeling of aircraft nose wheel steering system

The turning system of the forward landing gear system is mainly applied before the plane takes off and slide as well as the plane landed in taxi and exit, the system mainly includes the handwheel, pedal, enabling valve, by-pass valve, electro hydraulic servo valve (EHSV), steering control unit (SCU), turning actuating cylinder, linear variable differential transducer (LVDT), rotary variable differential transducer (RVDT) and related mechanical structure are composed of, the working principle of which is shown in Fig.1.

We know the plane turning system control principle from Fig.1, the pilot can through the handwheel (low speed) and pedal (generally used high-speed) to control the plane turning, then by RVDT, mechanical signals of handwheel and pedals are converted into electrical signals (voltage signals) and sent to the turning control unit. The turning control unit analyzes the electrical signals and send control signals (current signal) to the EHSV, EHSV controls the actual hydraulic fluid flow at both ends of the turning actuator cylinder to complete the landing gear turning action. The position feedback sensor is used to calculate the turning Angle and feedback the voltage signal to the turning control unit. The turning control unit compares the feedback signal with the control signal to obtain the error signal and send it to the EHSV in real time until the control Angle reaches the predetermined position.

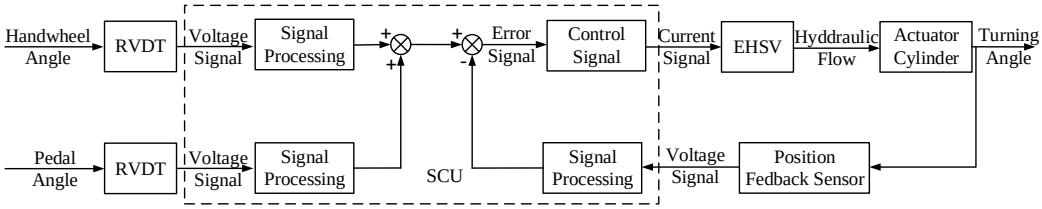

Fig. 1. The schematic diagram of aircraft nose wheel steering system

2.1 Manipulation module

The pilot can directly control the turning of the aircraft by handwheel and pedal. In normal turning action, the handwheel should be pressed down firstly to achieve the state of enabling the aircraft to turn, and the signal is transmitted to SCU by switch. Then the handwheel can be used to control the turning of the aircraft, and the mechanical action Angle of the hand wheel is ±80° and the mechanical motion Angle of the pedal is ±30°, which is shown in Fig.2. Normal mechanical action of the hand wheel will make the core of RVDT rotate, so as to induce different voltages and output them to SCU. The working principle of RVDT is shown in Fig.3.

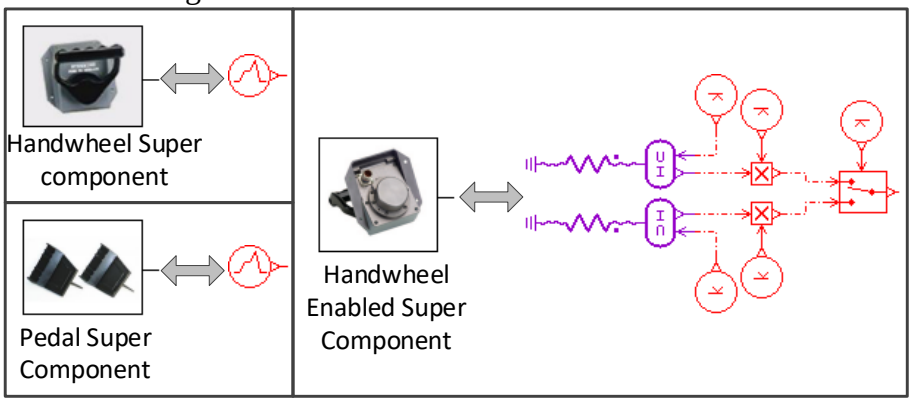

Fig. 2. Super component and models of handwheel and pedals

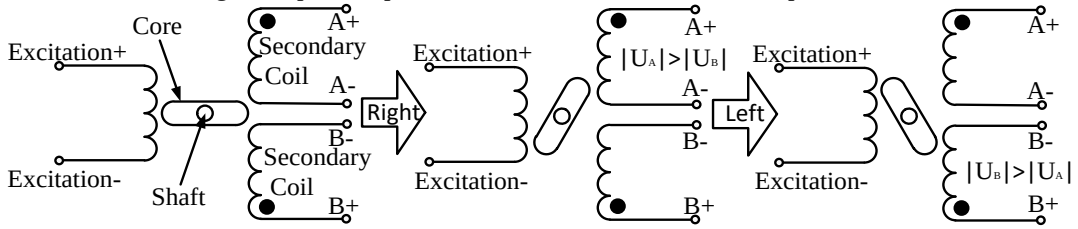

Fig. 3. Working principle of RVDT

The RVDT sensor is composed of a primary coil, two secondary coils and a rotatable iron core. Due to the different position and Angle of the iron core, the two secondary coils perceive the different voltage of the primary coil, so as to complete the purpose of converting mechanical signals into electrical signals[6-7]. The excitation voltage of the RVDT sensor under the handwheel and foot pedal is provided by SCU, which is shown as Formula (1).

$$V_{Exc}(t) = A_{Exc} \times \sin(2\pi f), \tag{1}$$

$V_{Exc}(t)$ is the excitation voltage of primary coil of RVDT; A_{Exc} is the peak-to-peak value of excitation voltage; f is the frequency of the excitation voltage.

Generally, the output of RVDT is determined by the difference between the effective voltage values of the two secondary coils, and the value is calculated by Formula (2).

$$V_O = V_{rmA} - V_{rmB} \cong P \times V_{rmExc} \times S + V_{rmExc} \times O, \tag{2}$$

V_O is the output of RVDT; V_{rmA} and V_{rmB} is the effective value of the induced voltage of the secondary coil. V_{rmExc} is the excitation of the primary coil; P is the actual position of the core of the RVDT; S is the sensitivity of the RVDT; O is the coefficient of variation between the two secondary coils of A and B.

Because of the difference of the upper and lower positions of the iron core, the voltage difference between the secondary coil is also different, and the result can be calculated by Formula (3).s

$$V_{ORVDT} = \frac{V_{rmA} - V_{rmB}}{V_{rmA} + V_{rmB}}, \tag{3}$$

V_{ORVDT} is the output of the RVDT.

The RVDT sensor in the model is shown in Fig.4. Port 2 is the SCU connected directly from the output Angle of the handwheel, and the voltage waveform converted from the mathematical model to the actual output to the SCU is used in the subsequent research on system-level design coordination and debugging in the manufacturing process.

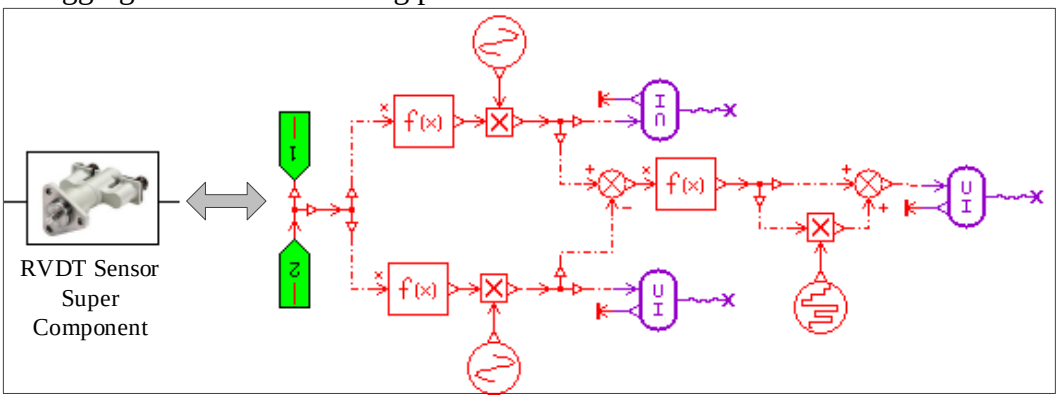

Fig. 4. The model of RVDT sensor

2.2 Control unit module

The normal steering control unit mainly has the functions of receiving driver's steering command, receiving and analyzing of sensor signals and other enabling signals, controlling the signals of bypass valve and electro-hydraulic servo valve, and exchanging information with other systems. The super component and model established by AMESim are shown in Fig. 5.

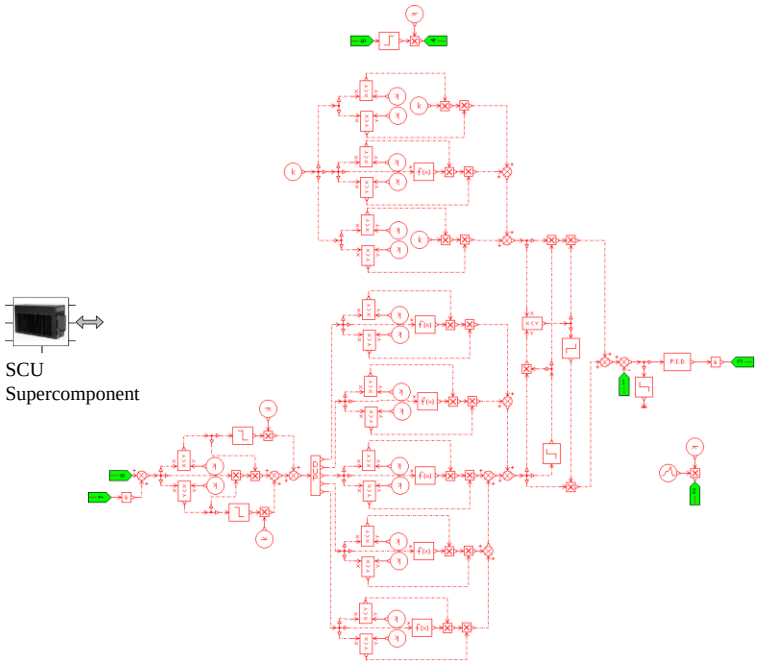

Fig. 5. The super component and corresponding model of landing gear control unit

Due to aircraft wheel mechanical Angle range in the range of ±80 °, and the plane turning Angle range in the range of ±66 °, thus the SCU rival wheel mechanical Angle calculation of relations as shown in Fig.6(a), and the maximum Angle the plane is allowed to turn is reduced as the speed increases to prevent the plane from turning over, the restriction relation of SCU to the maximum turning Angle of aircraft at different speeds is shown in Fig.6(b). Therefore, the main functions of this model are: the transformation of handwheel Angle and turning Angle, the restriction of aircraft operating speed on the maximum allowable turning Angle of aircraft, and the receiving and sending of enabling signals.

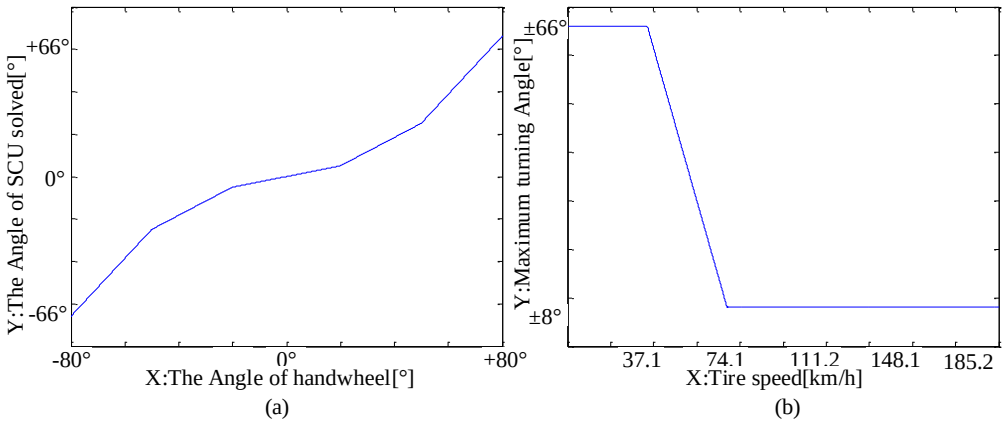

Fig. 6. The logical signal diagram in the SCU

2.3 Mechanical module

The nose landing gear adopts a pinion and rack steering gear in which the diameter of the gear is 80mm. The tire subjects to a lateral friction when turning the aircraft. The force of different steering Angles is different, so it is necessary to establish a mechanical model as shown in Fig. 7. For ease of analysis, the actuator has been subjected to a force of 6000N in the direction opposite to the direction of movement.

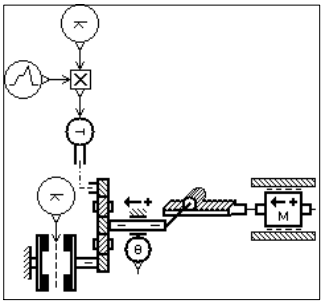

Fig. 7. The model of the stress of the plane turning

Position sensor is also an important sensor of turning system, the diameter of the gear in Fig.7 set to 80 mm, because there are an Angle sensor in AMEsim, we can directly figure out the Angle at which the plane turns, the actual position sensor working principle as shown in Fig.8, two secondary coil are normally placed at 90°, the landing gear and rotation Angle of position sensor gear ratio is 2.43:1, the relationship between the primary coil and secondary coil as shown in Formula (4).

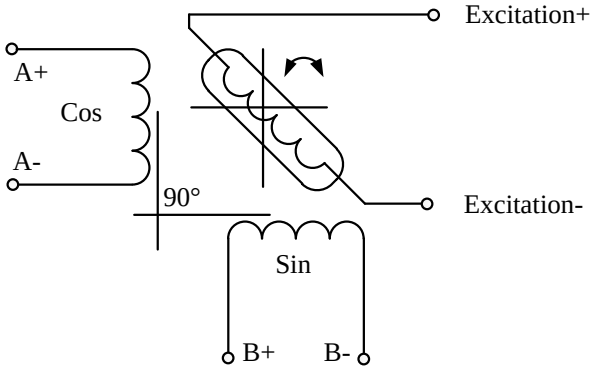

Fig. 8. Working principle of position sensor

$$\begin{aligned} E\left(Exc\right) &= N \times E\left(\mathrm{Sin}\right) \times \sin\left(\theta/2.43\right) \\ E\left(Exc\right) &= N \times E\left(\mathrm{Cos}\right) \times \cos\left(\theta/2.43\right) \end{aligned}, \tag{4}$$

2.4 Hydraulic module

The bypass valve is mainly opened under the influence of the pressure of the hydraulic system in the aircraft steering system. The model is shown in Fig.9. The enable valve is connected to the oil outlet in normal situation. When the signal is enabled, it connects to the oil inlet. The SCU only needs to control the enable valve, so that the bypass valve is pushed by the hydraulic oil. Since the valves in AMESim are all controlled by signals, the bypass valve super component is established to open when it detects the pressure on the A side of the enable valve. Because this paper does not do too much analysis on the electro-hydraulic servo valve, a three position four port hydraulic valve is used to replace the EHSV.

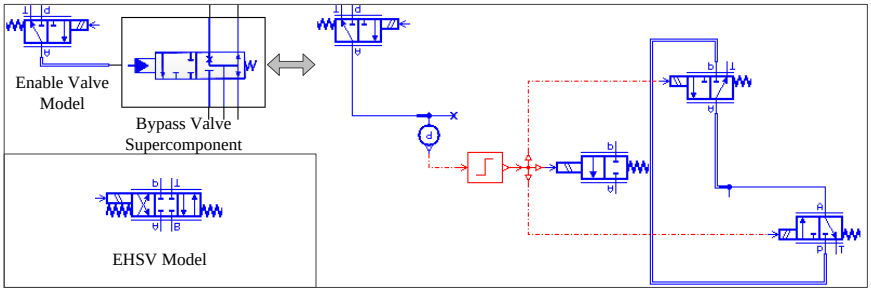

Fig. 9. The model of enable valve, bypass valve and EHSV

The opening of EHSV in aircraft turning system is detect by an LVDT sensor, its principle as shown in Fig.10, an LVDT sensor consists of a core can move up and down, a primary coil, two secondary coils, as the core position of up and down is different on both ends of the secondary coil induction voltage difference is different also, the final results as shown in Formula (5)[8-10].

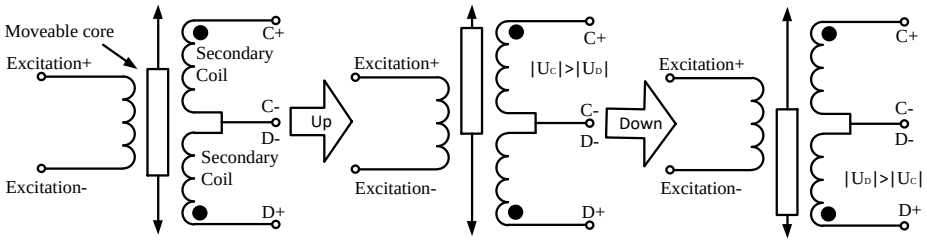

Fig. 10. Working principle of LVDT sensor

$$V_{OLVDT} = \frac{V_{rmC} - V_{rmD}}{V_{rmC} + V_{rmD}}, \tag{5}$$

V_{OLVDT} is the output value of the LVDT sensor calculated by SCU; V_{rmC}, V_{rmD} are the effective value of the induction voltage of the secondary coil.

The LVDT sensor model is established as shown in Figure.11. Since the opening degree of the EHSV model cannot be directly tested, the model uses the current of the EHSV to reflect different opening degrees. When the control

current changes from -8mA to +8mA, the change characteristics of the LVDT sensor's effective value are shown in Fig. 12.

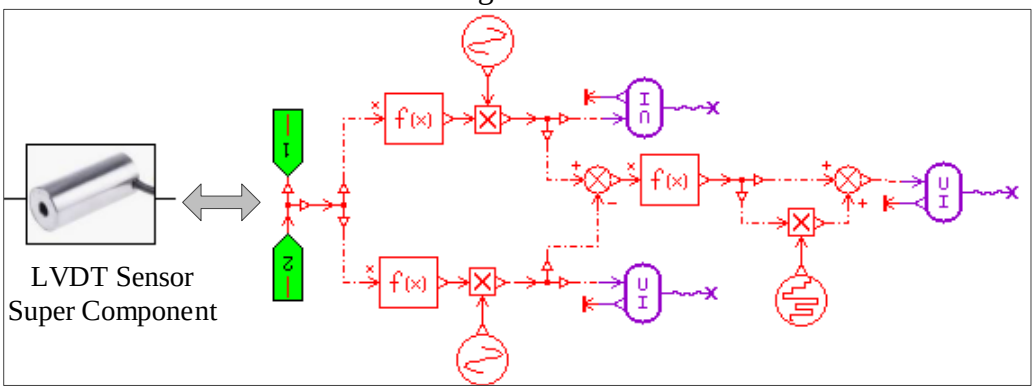

Fig. 11. The model and super component of LVDT sensor

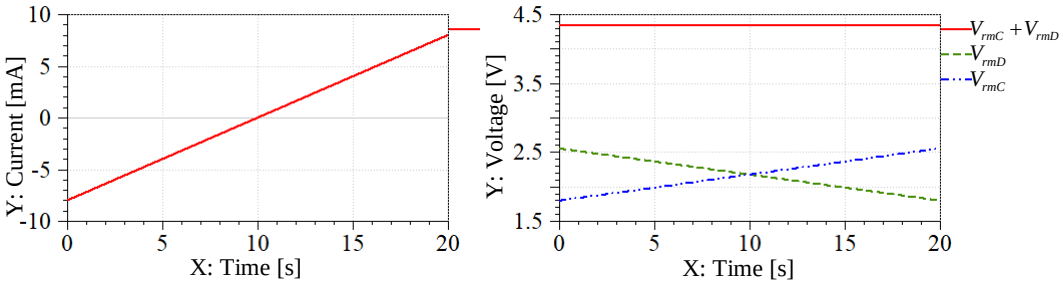

(a) The control current of EHSV (b) The output of the LVDT secondary coil

Fig. 12. The relationship between the output of LVDT and the control current of EHSV

The hydraulic models established based on the model's maintenance manual and related internal interface files. The relevant parameters of the nose wheel steering system are shown in Table 1.

Table 1

The parameters of related sub-models

Component Model	Title	Value	Unit
Hydraulic motor	Shaft speed	2700	rpm
Hydpump	Pump displacement	8	cc/rev
Oil out accumulator	Accumulator pressure	24000000	Pa
Return oil accumulator	Accumulator pressure	1200000	Pa
Relief valve	Creaking pressure	20684272	Pa
EHSV valve	Flow rate	0.000133	m^3/s
Enable valve	Flow rate	0.000033	m^3/s
Shimmy relief valve	Creaking pressure	23442175	Pa
Steering actuator	Piston diameter	0.025	m
	Rod diameter at left	0.012	m
	Rod diameter at right	0.012	m
	Displacement of piston	0.3	m

The final model of the turning system is shown in the Fig.13, which includes hydraulic part, turning part, control unit part, handwheel and pedal part, sensor part and actual turning moment part, etc.

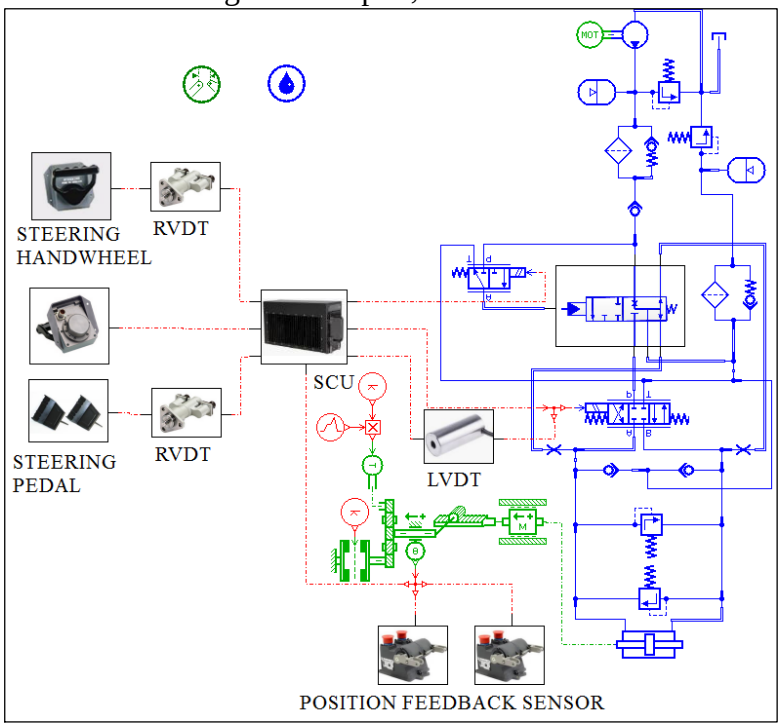

Fig. 13. The final model of turning system

The simulation time was set as 80s, in which the rotation Angle of the handwheel in the first 20s was changed from 0° to -80°, the rotation Angle of the handwheel in the middle 40s was changed from -80° to 80°, and the rotation Angle of the handwheel in the last 20s was changed from 80° to 0°, and the aircraft speed was set at 1km/h. After completion of the simulation, the simulation results were shown in Fig.14.

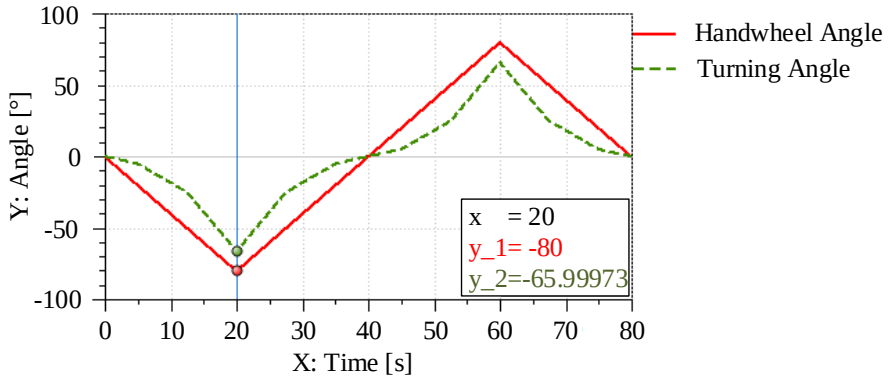

Fig. 14. Simulation diagram of turning system

When the taxiing speed of the aircraft is different, the allowed turning Angle of the aircraft is also different. By using the batch processing function of AMESim, the taxiing speed of the aircraft is set as 10km/h, 30km/h, 50km/h, 70km/h and 90km/h, and the handwheel or pedal movement is the same. The simulation results are shown in Fig.15.

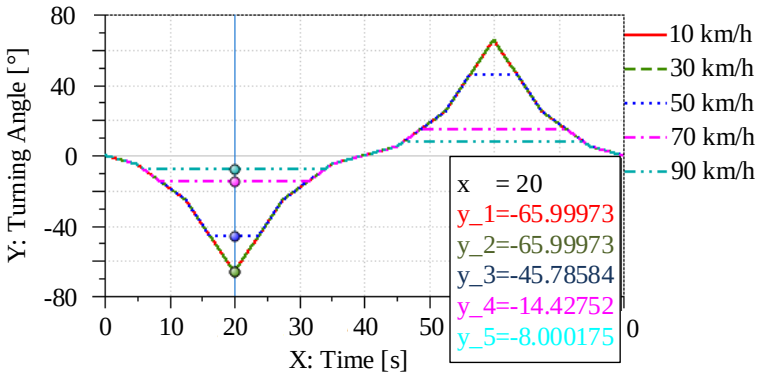

Fig. 15. Simulation results of different sliding speeds

3. Simulation under normal conditions

The aircraft turning system mainly works in two states: one is the high-speed state, which is mainly reflected in the takeoff and landing of the aircraft, in this state the aircraft turning is mainly controlled by the pedal. The other is the low speed state, which is mainly reflected in the ground control before takeoff and approach or after landing and exit. In this state, the turning of the aircraft is mainly controlled by hand wheel.

When airplane is at low speed, it is assumed that when the simulation arrives at 5S, the turning Angle of the handwheel is set to be 3.3°/s and the aircraft control speed is 1km/h for the convenience of observation and analysis. Moreover, when the simulation time goes from 5S to 25s, the handwheel Angle turns from 0° to -80°, from 25s to 65s from -80° to 80°, and finally from 65s to 85s, the handwheel Angle turns from 80° to 0°. By setting the model parameters of the turning system, we can get the variation trend of the mechanical Angle of the handwheel, the control current of the EHSV and the aircraft's turning Angle in this case as shown in the Fig.16. Due to space reasons, the variation trend of secondary variables such as RVDT coil output signal, LVDT coil output signal and position sensor output signal is not shown.

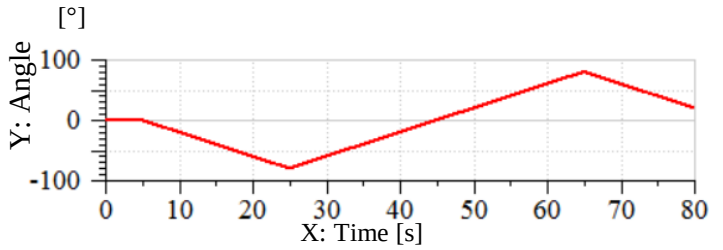

(a) Handwheel mechanical Angle

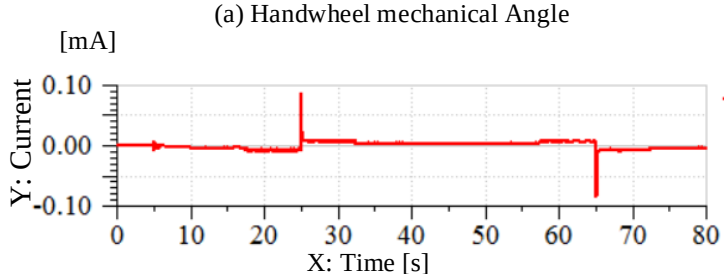

(b) EHSV control current

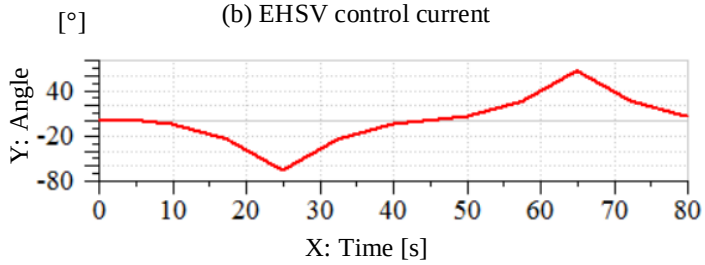

(c) Airplane turning Angle

Fig. 16. Signal variation during low speed

Generally, when the taxiing speed of the aircraft exceeds 80km/h, the turning can only be controlled by the pedal, and the mechanical Angle that the pedal can be manipulated is ±30°.In order to carry out the functional simulation of the turning system during the high-speed movement of the aircraft, the sliding speed of the aircraft in the model was set as 180km/h, and the mechanical angular speed controlled by the pedal was set as 3°/s. The input of the pedal was changed from 0° to -30° from 0s to 10s, from -30° to 30° from 10s to 30s, and from 30° to 0° from 30s to 40s. By setting the model parameters of the turning system, we can get the variation trend of the mechanical Angle of the handwheel, the control current of the EHSV and the aircraft's turning Angle in this case as shown in the Fig.17. Due to space reasons, the variation trend of secondary variables such as RVDT coil output signal, LVDT coil output signal and position sensor output signal is not shown.

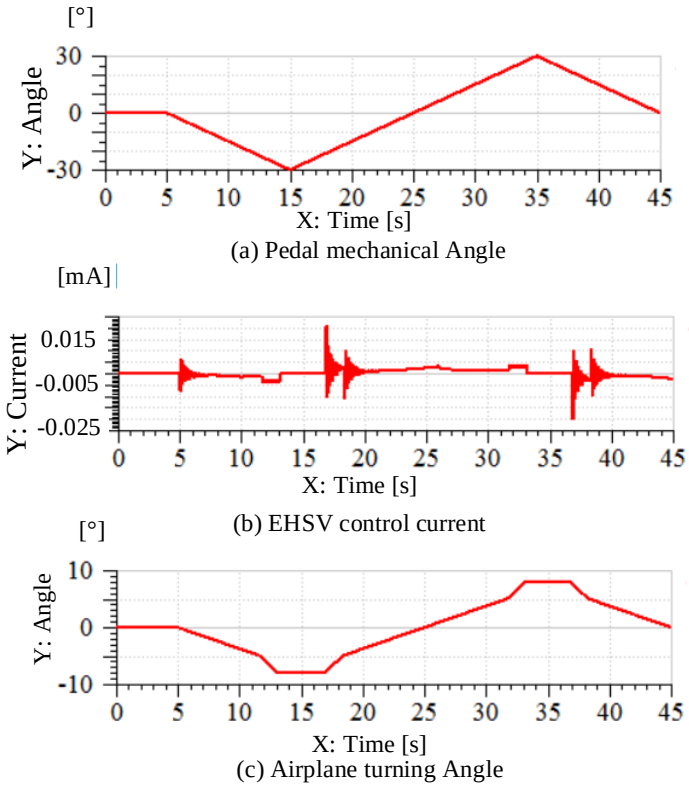

(a) Pedal mechanical Angle

(b) EHSV control current

(c) Airplane turning Angle

Fig. 17. Signal variation during low speed

4. Simulation under fault conditions

For joint debugging between systems in the design stage, it is necessary not only to run functional simulation when the steering system is in normal state, but also when the steering system is in abnormal state. Common failures of the steering system include: actuator leakage, component wear and deflection jitter. This section mainly analyzes the leakage of the steering actuator and the leakage of the electro-hydraulic servo valve. It not only analyzes the failure mechanism, but also simulates and analyzes the electrical signals of the actual aircraft steering system, which is of great significance for system design and manufacturing debugging in the future.

4.1 The leakage of the steering actuator

After the aircraft has made multiple turns, the sealing ring of the steering actuator will show some damage and cause leakage. Different leakage levels will cause different changes in the steering performance of the aircraft. Through the AMESim batch processing function, the leakage volume was set as 0L/min/bar

and 0.06L/min/bar for functional simulation. The input conditions are the same as in the normal state, and the simulation results are as shown in the Fig.18.

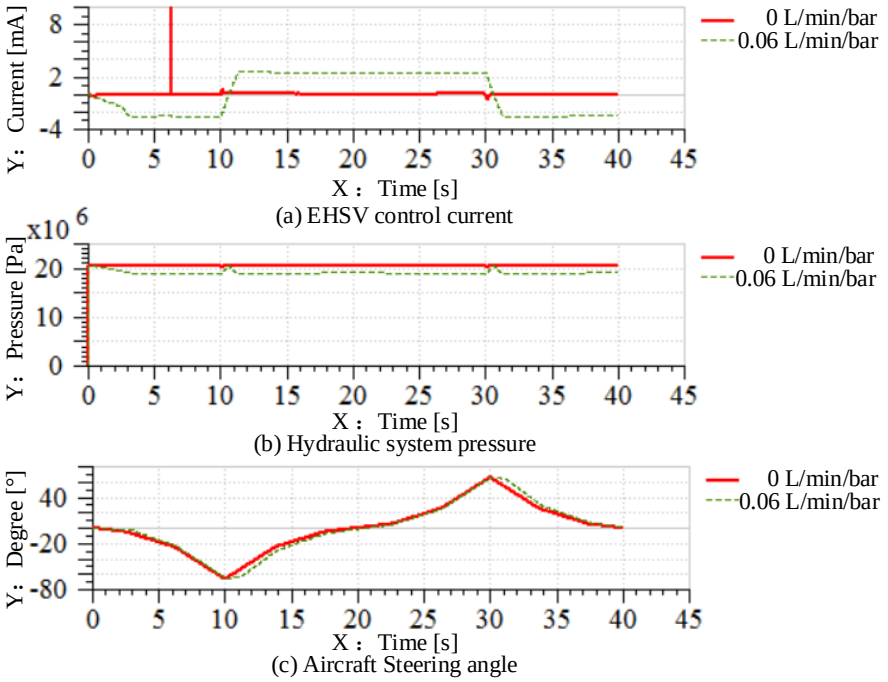

Fig. 18. The diagram of electrical signals when the actuator leaks

The control signal of the electro-hydraulic servo valve is gradually increasing as shown in the Fig.18(a), and the pressure value of the hydraulic system is also slightly changed as shown in the Fig.18(b).

By analyzing the signal of the aircraft steering angle in the model as shown in Fig. 18(c), we know that although it can still meet the needs of steering maneuvering, it produces a certain delay. Because of the low angular velocity during steering maneuvering, a larger delay will occur when increasing the angular steering velocity.

4.2 The leakage of the electro-hydraulic servo valve

The electro-hydraulic servo valve is an important component of the steering system. It is directly controlled by the SCU, and the flow control of hydraulic system is completed by controlling the torque motor coil. The electro-hydraulic servo valve will have faults such as jamming, sealing ring failure, and internal device corrosion. Faults such as jamming and internal device corrosion can be clearly shown, but leakage problems such as sealing ring failure are difficult to find. In order to better analyze its leakage failure, use AMESim to set the leak gap diameter to 0mm and 1.54mm for functional simulation. It provides

some reference for the purpose of fault diagnosis by comparing flight data with model data in the future. The error between the model data and the flight data can be used to modify the model. The input conditions are the same as in the normal state, and the simulation results are as shown in the Fig.19.

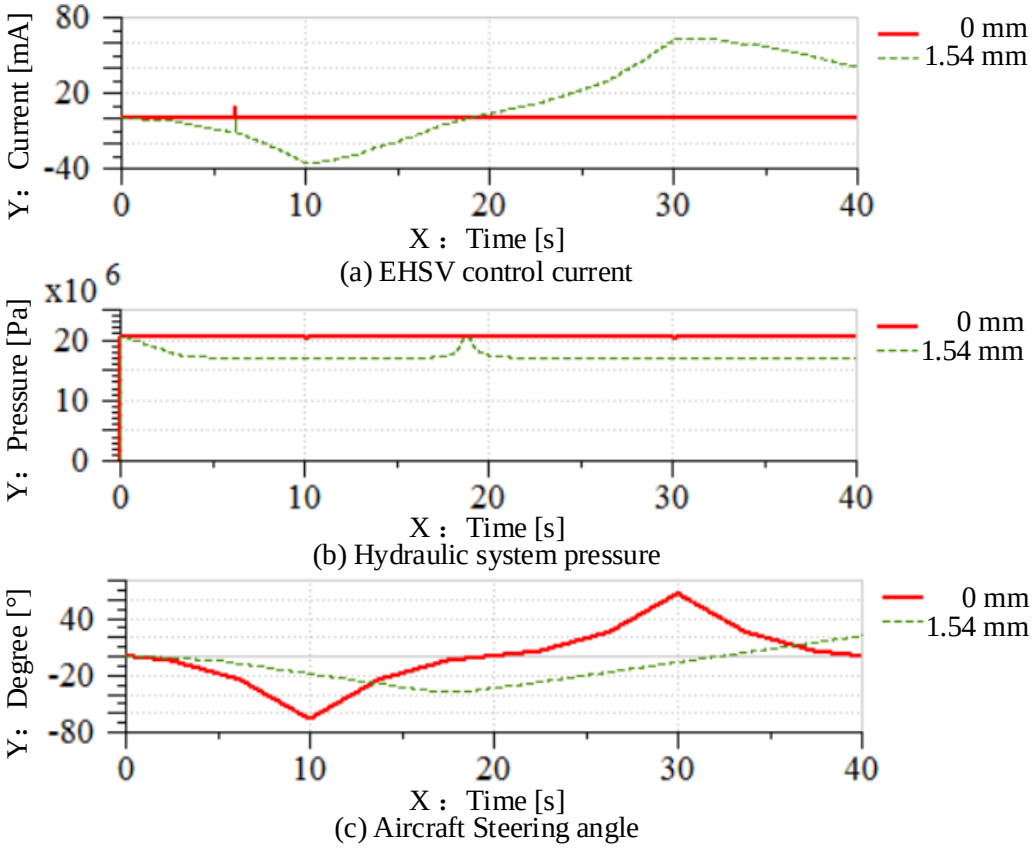

Fig. 19. The diagram of electrical signals when the EHSV leaks

The control current of the electro-hydraulic servo valve is ± 8mA. But the control current of the electro-hydraulic servo valve has reached the maximum and cannot continue to adjust as shown in the Fig.19(a). The signal of the position feedback sensor is abnormal. The pressure of the hydraulic system has also dropped as shown in the Fig.19(b). In fact, the angle sensor in the model found that the aircraft was no longer able to control the steering normally as shown in Fig.19(c). The force generated by the steering action on the rod is shown by Formula (6).

$$f_{rod} = p_1 \cdot A_1 - p_2 \cdot A_2 + v \cdot visc, \tag{6}$$

f_{rod} is the force exerted by the rod due to the pressures and viscous friction; A_1 is the annular area of the piston on which pressure is p_1; A_2 is the annular area

on which pressure is p_2; v is the moving speed of the cylinder piston; *visc* is the viscous friction of hydraulic oil.

Since the viscous friction force is not considered in this paper, when the pressure drops to a certain level, the steering moment of the aircraft cannot overcome the lateral force of the aircraft tire, then the aircraft out of control.

5. Conclusions

This paper uses AMESim to simulate and model a certain type of aircraft steering system. We have simulated the trends of electrical signals when the system is working normally and abnormally. Then, we analyzed the reason for the failure and come to the following conclusions.

1. According to the corresponding relationship between handwheel angle and aircraft steering angle in the manual and the maximum allowable steering angle of the aircraft at different wheel speeds, the accuracy of the steering system model was verified. Then, the simulation of the electrical signals under normal conditions also meets the manual's requirements. Therefore, it is of great significance to make the relevant system and the normal steering system jointly debug to achieve verification.

2. The steering system model can be used to conduct fault analysis and reflect various fault factors through electrical signals. The leakage of actuator and electro-hydraulic servo valve are analyzed, and the variation trend of electrical signals is simulated. Therefore, it is of great significance to make the relevant system and the abnormal steering system jointly debug to achieve verification.

Acknowledgments

This study is supported by the Fund of National Engineering and Research Center for Commercial Aircraft Manufacturing (COMAC-SFGS-2019-343), the Training Plan of Tianjin University Innovation Team (Grant No.TD13-5071) and the Basic Scientific Research Project of the Central University (3122019042).

R E F E R E N C E S

[1]. *Pavan M S, Vyas J J and Balamurugan G*, Modelling and simulation of aircraft nose wheel steering system, 2015 39th National Systems Conference (NSC), Noida, 2015, pp. 1-5.

[2]. *Robert S*, Aircraft Level Steering Runaway Failure Analysis (2009-01-3136), in Advances in Aircraft Landing Gear, SAE, 2015, pp.65-70.

[3]. *Mohsen R and Kamran B*, Investigation on the effect of coulomb friction on nose landing gear shimmy, Journal of Vibration and Control, 2018, vol 25. 255-272.

[4]. *Infante V, Fernandes L, Freitas M*, Failure analysis of a nose landing gear fork, Journal of Engineering Failure Analysis, 2017, 82, 554-565.

[5]. *Hu Y G, Zhang Q, and Wang X P*, Oil Leakage Failure Analysis and Improved Design on Front Wheel Turning Actuating Cylinder of an Aircraft, Journal of Lubrication Engineering, 2013, 38(10): 99-101.
[6]. *Li G X and Huang R C,* Application of RVDT sensor in rudder Skewness measurement of Aircraft, China Science and Technology Information, 2017(08): 22-23.
[7]. *Wei T and Xia D T,* Research of AC Analog Modulated Based on LVDT/RVDT, Aeronautical Computing Technique, 2013, 43(01): 116-119
[8]. *Cha T and Ding Y X,* Application and Analysis of Filtering in LVDT Conditioning Circuit, Journal of Wuhan Polytechnic, 2019, 18(04): 94-98.
[9]. *Jiang C, Peng L Z and Sun J G,* Signal processing and on-line failure monitoring of LVDT sensor on aero-engine control system, Journal of Aerospace Power, 2007(08): 1396-1400.
[10]. *Zhang J L and Pan H H,* Effect of secondary coil winding taper on static characteristics of LVDT, Manufacturing Technology & Machine Tool, 2019(11): 135-138+142.